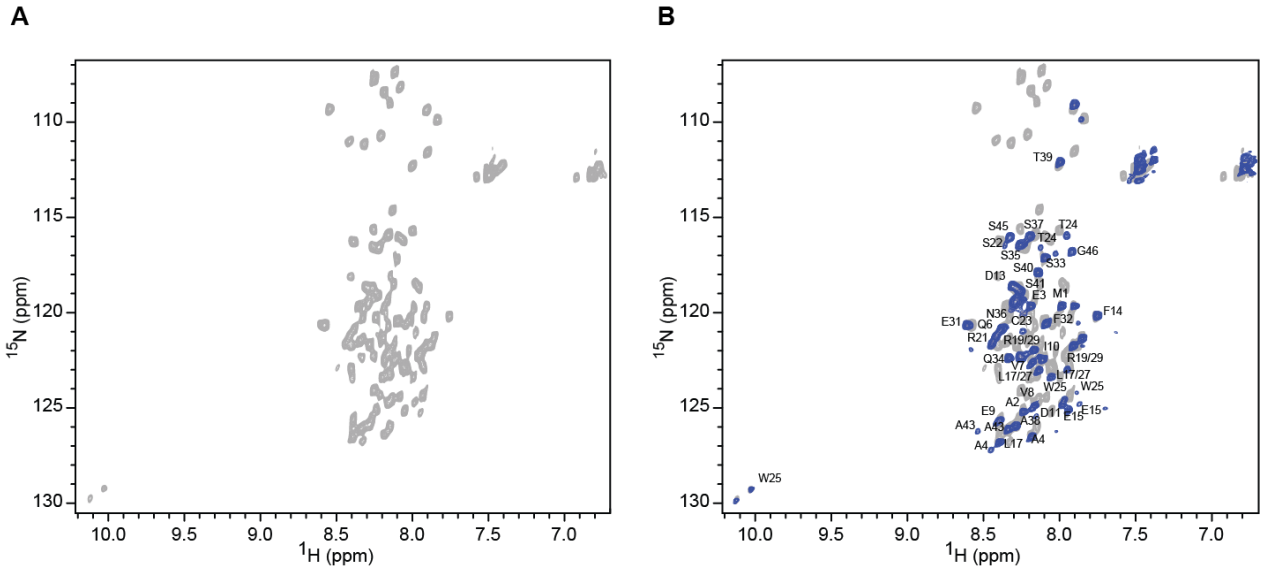

Figure S1. Comparison of 2D ^{1}H/^{15}N HMQC spectra of NTDΔ with the full length NTD (A) 2D ^{1}H/^{15}N HMQC spectra of FOXO1´s NTD. Complete assignment of all amino acids was not possible due to overlaps of chemical shifts. **(B)** All ^{1}H/^{15}N chemical shifts are collapsed around 7.5 – 8.5 ppm in the ^{1}H dimension, for superimposed spectra of full length NTD (grey) and NTDΔ (blue), indicative of an overall disordered nature of both proteins.

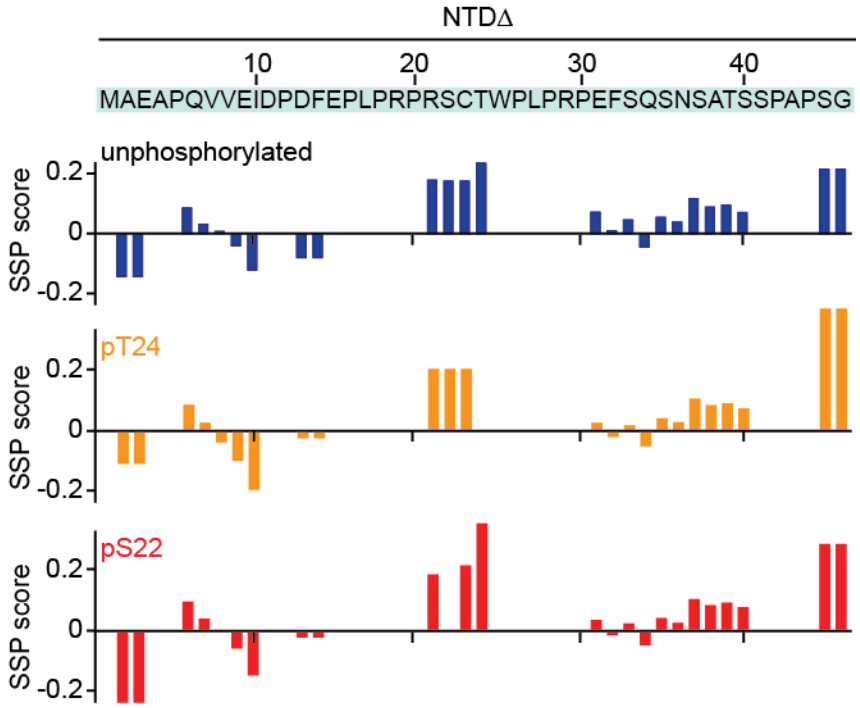

Figure S2. Secondary structure propensity of NTDΔ Secondary structure propensity (SSP) scores for NTDΔ in different phosphorylation states based on the Cα and Cβ chemical shifts with five-residue weighted averaging. Positive scores indicate an α-helix and negative scores suggest a β-sheet propensity. Prolines and amino acids directly preceding prolines were excluded in the SPP analysis as they are not visible in the $^{1}H/^{15}N$ HMQC spectra. The unphosphorylated NTDΔ (shown in blue) contains a largely unstructured character with weak α-helical propensities for amino acids 21-25 (average SSP score of 0.19), a region mediating 14-3-3 interactions. Additionally, amino acids 35-40 had an average score of 0.08, also indicating a weak α-helical propensity. Yet, the overall SSP scores of NTDΔ suggested a predominantly unfolded polypeptide chain. The SSP scores of NTDΔ-pT24 (shown in orange) and NTDΔ-pS22 (shown red) were overall comparable to the unphosphorylated NTDΔ, showing no detectable structural changes upon phosphorylation.

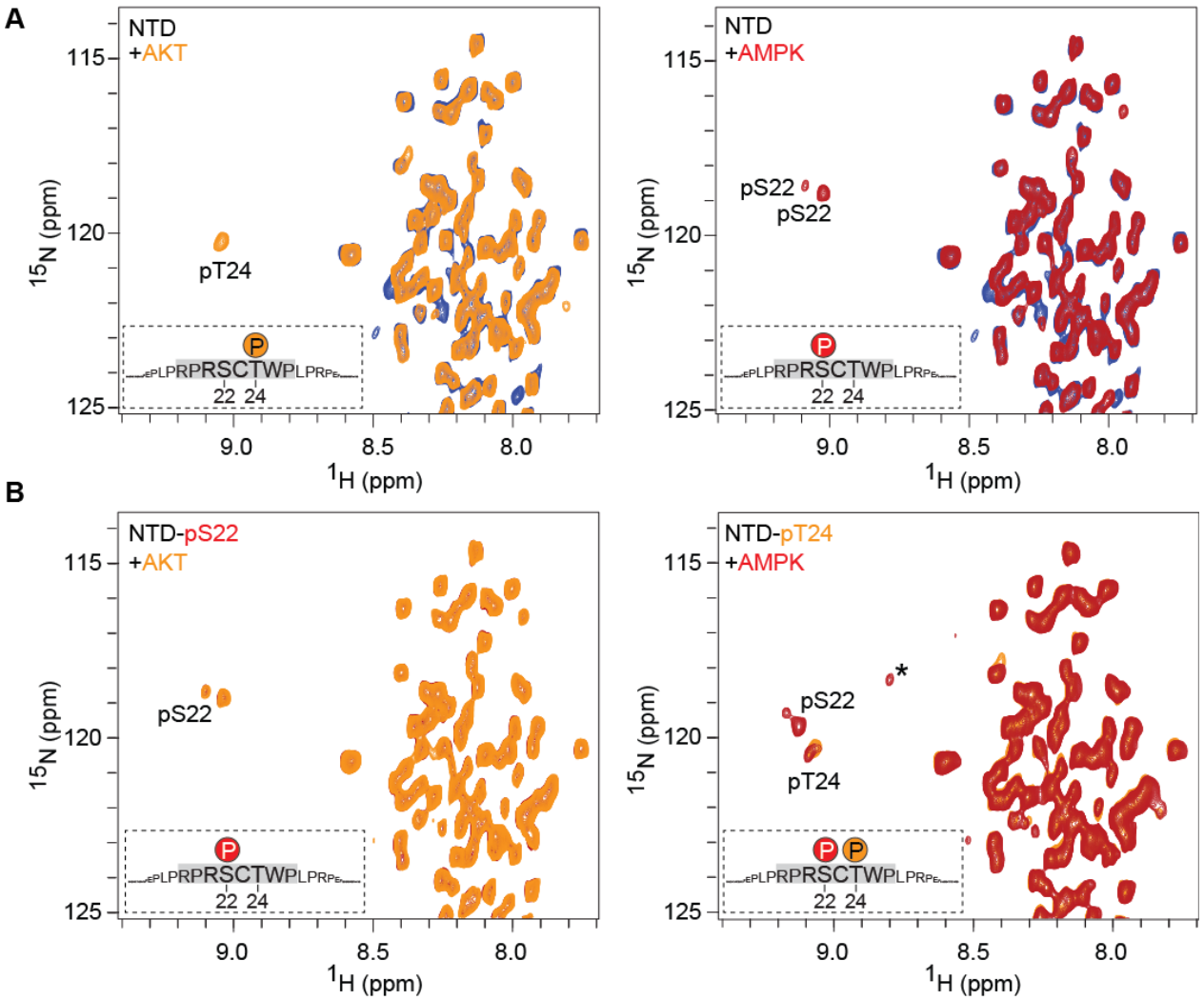

Figure S3. Phosphorylation of the NTD by AKT and AMPK (A) 2D $^{1}H/^{15}N$ HMQC NMR spectra of the NTD incubated for 3 h with purified AKT (in orange) or AMPK (in red) to assess T24 and S22 phosphorylation by AKT and AMPK, respectively. Two peaks for pS22 indicate dual conformations. **(B)** 2D $^{1}H/^{15}N$ HMQC NMR spectra of the pre-phosphorylated NTD incubated with the indicated kinases for 4.5 h. NTD-pS22 with AKT to monitor T24 phosphorylation (in orange) and NTD-pT24 with AMPK to analyze S22 phosphorylation (in red). AMPK phosphorylated S22 on NTD-pT24 while AKT could not phosphorylate T24 on NTD-pS22 as observed for the truncated NTD (NTDΔ). Additionally, a weak peak appeared at 8.78/118.35 ($^{1}H/^{15}N$) ppm when NTD-pT24 was incubated with AMPK indicated by an asterisk. Peptide mapping by LC-MSMS revealed that either S62 or S72 was also weakly phosphorylated by AMPK.

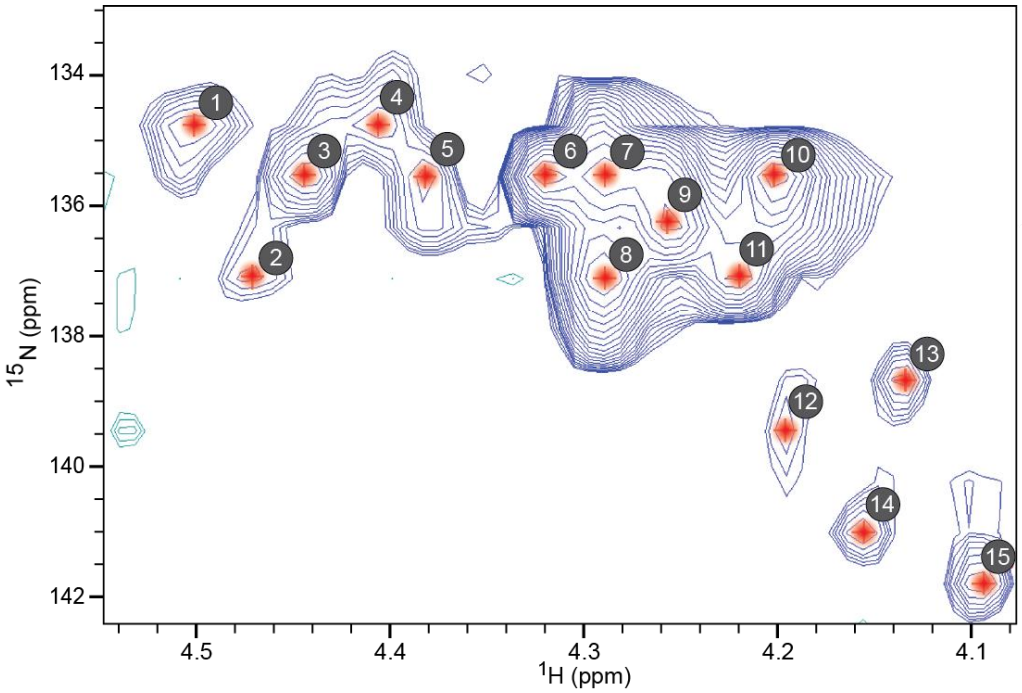

Figure S4. Isomerization analysis of prolines in NTDΔ Two-dimensional Hα(Cα)N NMR projections of $^{15}N/^{13}C$-doubly labeled NTDΔ centered on the Hα/N region of proline residues. 15 Hα/N peaks were identified by automatic peak-picking. NTDΔ contains 10 prolines suggesting that at least five prolines are present in both cis and trans conformations.

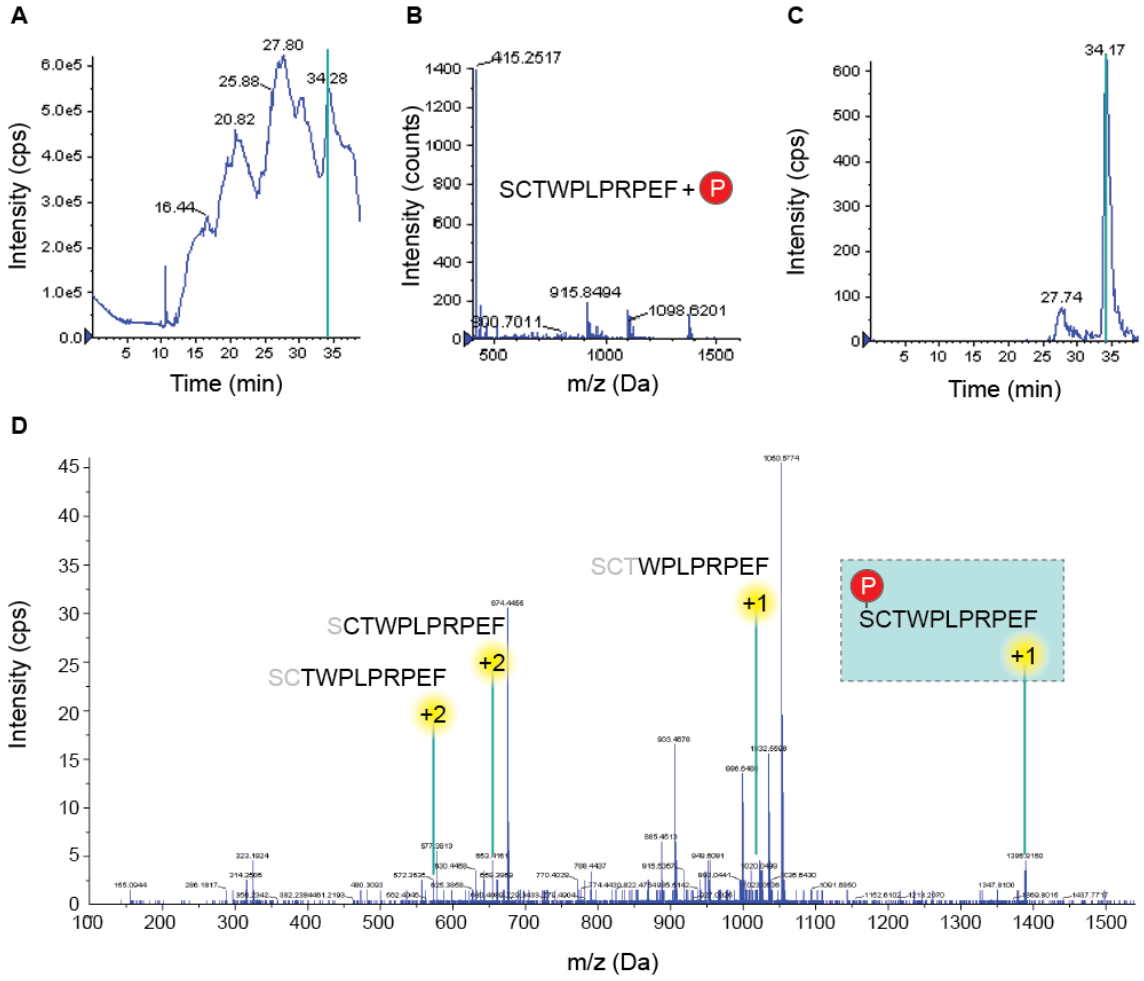

Figure S5. Analysis of phosphorylation sites of AMPK in the NTD of FOXO1 by LC-MSMS (A) Total ion count chromatogram of the digested NTD incubated with AMPK. **(B)** M/z spectra of phosphorylated peptide fragments (MS). **(C)** Extracted ion count chromatogram. **(D)** m/z spectrum of product ions (MSMS). The peptide fragments corresponding to double charged TWPLPRPEF and CTWPLPRPEF suggested that S22 has been the site of phosphorylation.

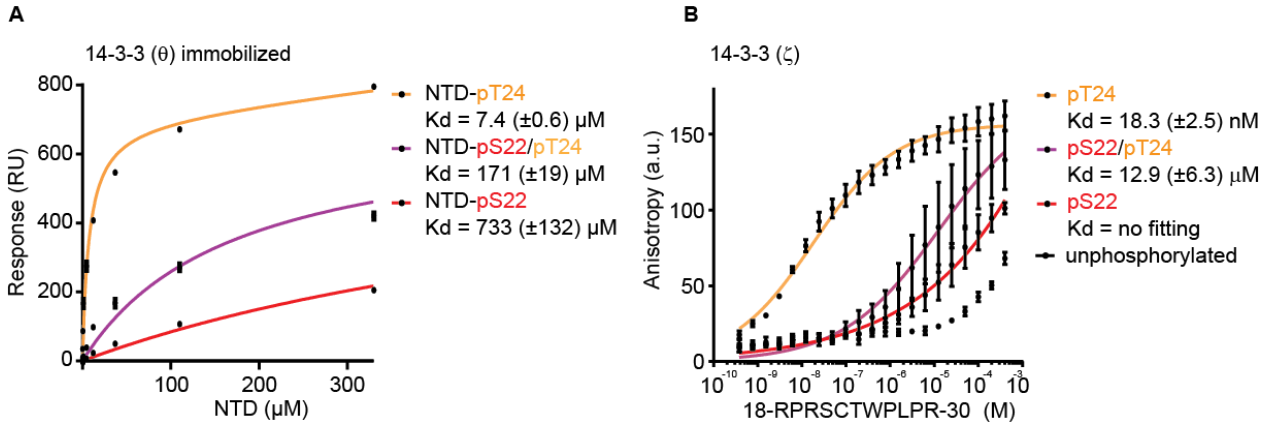

Figure S6. Phosphorylation of S22 in the NTD of FOXO1 prevents 14-3-3 interactions (A) Surface plasmon resonance (SPR) binding analysis of 14-3-3 θ and the NTD of FOXO1 phosphorylated at the indicated residues. NTD-pT24 served as positive control and the unphosphorylated NTD was used as linear component for data correction. Data are expressed as mean ± SD of technical triplicates from one representative experiment. **(B)** Fluorescence Anisotropy binding analysis of interactions between 14-3-3 ζ and the FOXO1 peptide (18-RPRSCTWPLPR-30) in different phosphorylation states. Data are expressed as means ± SD from three independent experiments and fitted with Prism (Specific binding with Hill slope).

A

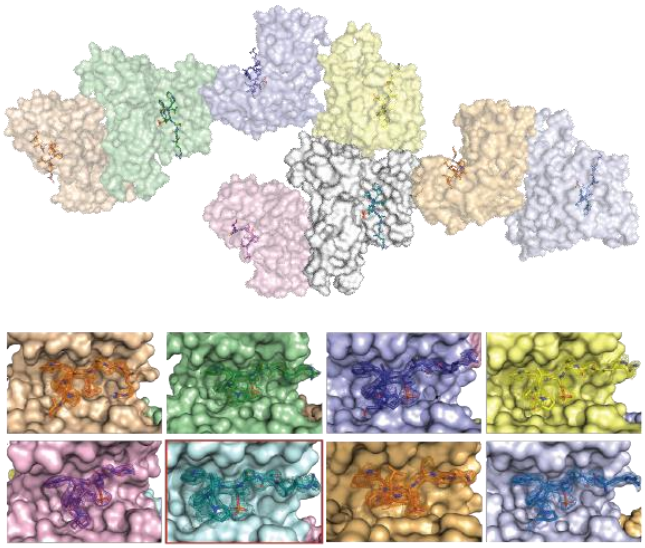

B

FOXO1-pT24 in complex with 14-3-3 σ

Probable space groups	P 21
Unit cell	149.21, 62.81, 154.04, 90.00, 103.24, 90.00 Å
Lower res.	119.09 (2.34) Å
High res.	2.3 (2.3) Å
I/sigI	10.8 (3.8)
Completeness	100.0 (99.7) %
Anom Compl	99.6 (99.3) %
Rmerge	0.093 (0.390)
Multiplicity	6.5 (6.6)
Anom. Mult.	3.3 (3.4)
#Obs	810231 (40686)
#Unique	124223 (6125)

C

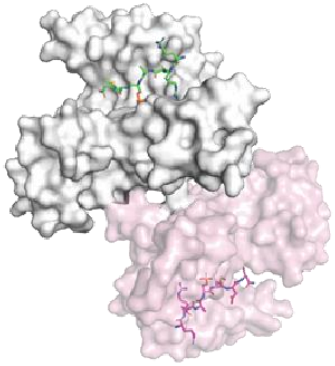

D

FOXO1-pS256 in complex with 14-3-3 σ

Probable space groups	P 21 21 21
Unit cell	63.43, 104.62, 156.87, 90.00, 90.00, 90.00 Å
Lower res.	58.80 (1.93) Å
High res.	1.90 (1.90) Å
I/sigI	13.02 (1.71)
Completeness	100.0 (97.2) %
Anom Compl	99.9 (97.2) %
Rmerge	0.105 (0.847)
Rpim (separate Friedels)	0.044 (0.408)
Rpim (pooled Friedels)	0.032 (0.244)
Rmeas (pooled Friedels)	0.113 (0.771)
Multiplicity	12.7 (10.6)
Anom. Mult.	6.6 (5.4)
#Obs	1053950 (42317)
#Unique	83148 (4011)

Figure S7. Detailed overview of the crystal structures obtained for FOXO1-pT24 and FOXO1-pS256 in complex with 14-3-3 σ (A) Crystal structure of FOXO1-pT24 in complex with 14-3-3 σ. Shown is the asymmetric unit with eight 14-3-3 monomers (surface representation) and the peptide (stick representation). **(B)** Crystallographic data collection and refinement statistics for FOXO1-pT24 in complex with 14-3-3 σ. **(C)** Crystal structure of FOXO1-pS256 in complex with 14-3-3 σ. Shown is the asymmetric unit with two 14-3-3 monomers (surface representation) and the peptide (stick representation). **(D)** Crystallographic data collection and refinement statistics for FOXO1-pS256 in complex with 14-3-3 σ.

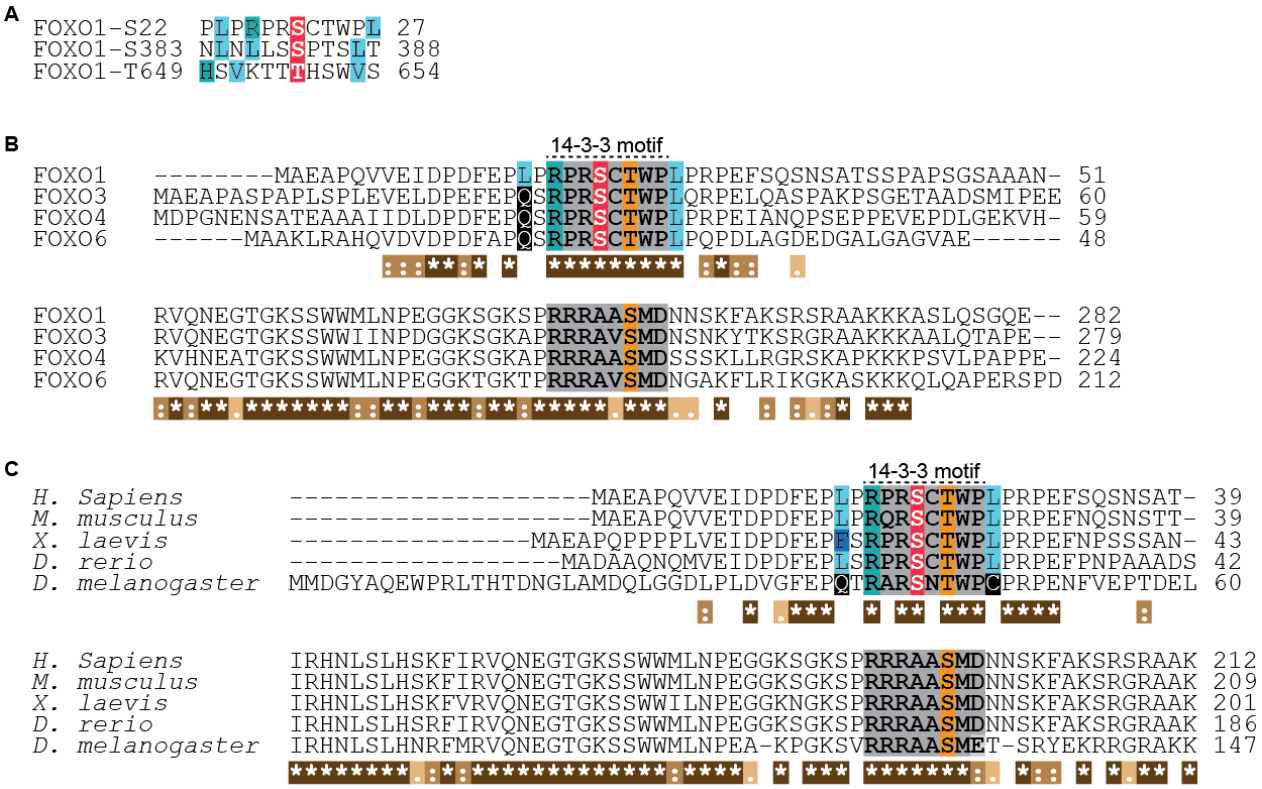

Figure S8. The AMPK recognition motif in the N-terminal 14-3-3 binding site is conserved in vertebrates (A) Alignment of the characterized AMPK phosphorylation sites in human FOXO1 (S22, S383, T649). Basic amino acids are shown in dark blue and hydrophobic residues in light blue. The AMPK phosphorylation sites are highlighted in red. **(B)** Alignment of the 4 human FOXO proteins. While the phosphorylation site corresponding to S22 and the leucine at position -5 as well as arginine at position +3 are conserved in all proteins, the leucine at position +5 is a unique feature of FOXO1. In other FOXO proteins the hydrophobic leucine is exchanged to a polar glutamine. Both 14-3-3 interaction motifs are highly conserved between all FOXO proteins (in grey). The known AKT phosphorylation sites corresponding to T24 and S256 in FOXO1 are shown in orange. Conserved amino acids are labeled with an asterisk and residues with similar properties are indicated in brown. **(C)** Alignment of FOXO proteins from commonly used model organisms. For species expressing multiple FOXO proteins the homolog of human FOXO1 was used. The residues corresponding to S22 in human FOXO1 is conserved (shown in red), however, the AMPK recognition motif is only conserved in vertebrates (shown in blue). Of note, in *Xenopus laevis* the leucine at position -5 is changed to phenylalanine, another hydrophobic residue. The known AKT phosphorylation sites corresponding to T24 and S256 in human FOXO1 are shown in orange. Conserved amino acids are labeled with an asterisk and residues with similar properties are indicated in brown.

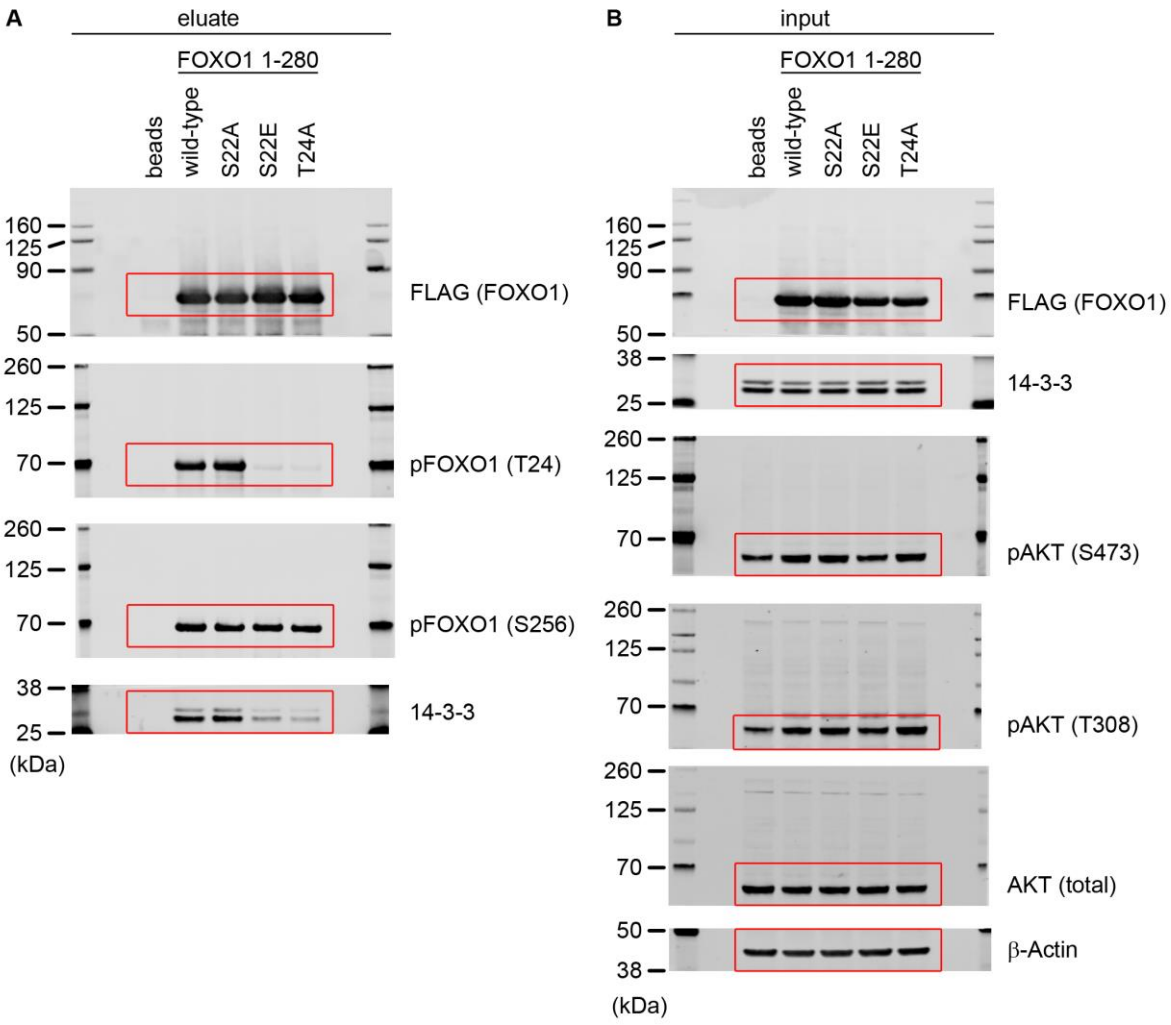

Figure S9. Uncropped immunoblots of Figure 4 (A) Western blot scans of the eluates from the immunoprecipitation. **(B)** Uncropped western blot scans of input samples. Cropped areas are indicated by red boxes. The Chameleon Duo Pre-stained Protein Ladder from LI-COR (#928-60000) was used to monitor molecular weights in the near-infrared channels (700 nm and 800 nm).